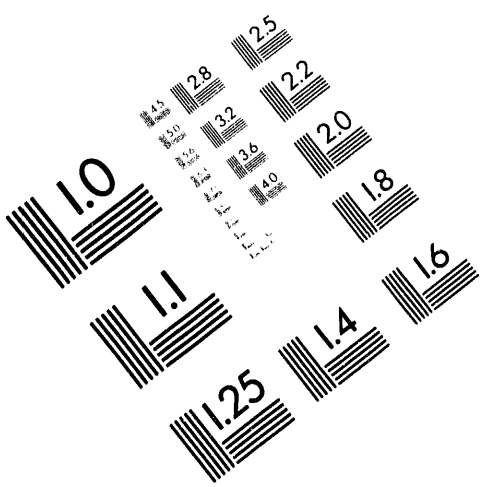

Association for Information and Image Management

1100 Wayne Avenue, Suite 1100
Silver Spring, Maryland 20910

301/587-8202

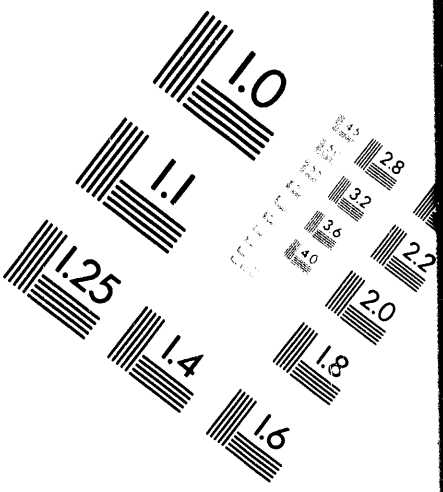

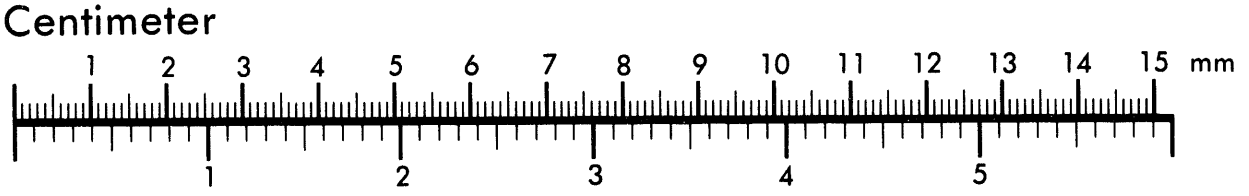

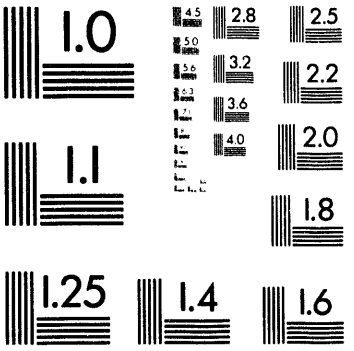

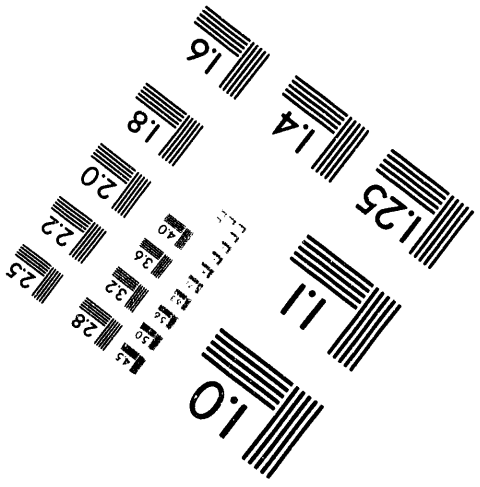

MANUFACTURED TO AIIM STANDARDS
BY APPLIED IMAGE, INC.

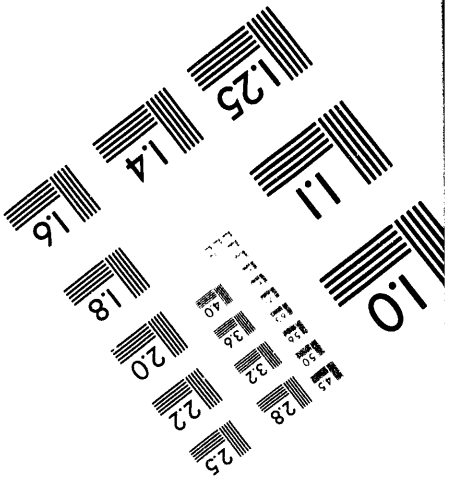

1 of 1

LBL-35559
UC-400

Experimental Study of Premixed Flames in Intense Isotropic Turbulence

B. Bédat and R. K. Cheng

Combustion Group
Energy & Environment Division
Lawrence Berkeley Laboratory
Berkeley, CA 94720

April 1994

This work was supported by the Director, office of Energy Research, Office of Basic Energy Sciences, Chemical Sciences Division of the U. S. Department of Energy under Contract No. DE-AC-03-76SF00098.

Experimental Study of Premixed Flames in Intense Isotropic Turbulence

B. Bédat and R. K. Cheng

Combustion Group
Energy & Environment Division
Lawrence Berkeley Laboratory
Berkeley, CA 94720

Abstract

A methodology for investigating premixed turbulent flames propagating in intense isotropic turbulence has been developed. The burner uses a turbulence generator developed by Videto and Santavicca and the flame is stabilized by weak-swirl generated by air injectors. This set-up produces stable premixed turbulent flames under a wide range of mixture conditions and turbulence intensities. The experiments are designed to investigate systematically the changes in flame structures for conditions which can be classified as wrinkled laminar flames, corrugated flames and flames with distributed reaction zones. Laser Doppler anemometry and Rayleigh scattering techniques are used to determine the turbulence and scalar statistics. In the intense turbulence, the flames are found to produce very little changes in the mean and rms velocities. Their flame speed increase linearly with turbulence intensity as for wrinkled laminar flames. The Rayleigh scattering pdfs for flames within the distributed reaction zone regime are distinctly bi-modal. The probabilities of the reacting states (i.e. contributions from within the reaction zone) is not higher than those of wrinkled laminar flame. These results show that there is no drastic changes in flame structures at Karlovitz number close to unity. This suggest that the Klimov-Williams criterion under-predicts the resilience of wrinkled flamelets to intense turbulence.

Introduction

The concept of premixed turbulent flames that burn within distributed reaction zones was introduced in the 1950s [1,2], the idea evolving from the pioneering work of Damköhler [3] on wrinkled laminar flames. Since then various criteria to differentiate the regimes of premixed turbulent flames have been postulated. The regimes are usually expressed on phase diagrams as functions of non-dimensional quantities that can be derived from the mixture properties and turbulence time and length scales [4-6]. These non-dimensional quantities are the turbulent Reynolds number, Re_t, the Damköhler number, Da and the Karlovitz number, Ka. Figure 1 shows Borghi's version which is also known as the Borghi-Barrère diagram. The underlying assumption of this and all the other phase diagrams is that the scaling laws for isotropic turbulence are required to relate Da and Ka to Re. Accordingly, $Da = (l_t/d_L)\,(u'/S_L)^{-1}$ and $Ka = (u'/S_L)^{3/2}\,(l_t/d_L)^{-1/2} = (d_L/l_k)^2$ [6]. The reaction zone thickness, d_L is defined by the original Klimov criterion $d_L\,S_L = \nu$. The Ka = 1 boundary, generally known as the Klimov-Williams criterion, separates the regimes of wrinkled laminar flames that have thin reaction zones from flames with thicker distributed reaction zones.

To date the majority of premixed turbulent flame experiments have been conducted within the wrinkled laminar flame and corrugated flame regimes. There have been only a few attempts [7-9] to validate experimentally the Klimov-Williams criterion. To achieve the necessary flow and flame conditions for the distributed reaction zones, Gökalp et. al. [7] developed an experiment using cool flames with very low heat release rates. They observed a broadened flame zone due to the penetration of small eddies. These conditions are more difficult to achieve in typical hydrocarbon flames. Furukawa et. al.[8] using intense turbulent jet flames, varied the relative velocity between the fuel/air jet and the co-flow to attain high turbulence levels and the analysis was based on the probability density functions (pdf) of ion-probe currents. They concluded that their low Damköhler number flames exhibit flamelet-like behavior. Yoshida et. al. [9] developed a burner that stabilized an annular flame between two plates and intense turbulence was generated by impinging two opposed jets at the plate centers. As in the work of Furukawa et. al.[8], the flames were subjected to shear type turbulence. Thermocouples, schlieren imaging and chemiluminescence emissions of C_2, OH and CH were used to characterize the flame structures. Although their thermocouple pdfs and the schlieren images show some non-flamelet like features, these data are open to different

interpretation. Whether or not combustion took place in distributed reaction zone remains inconclusive.

The main challenge in experimental work to verify the Klimov-Williams criterion is in generating and sustaining intense turbulence in the approach flow. Turbulence generated by a grid or a perforated plate is not very intense and dissipates quickly. The alternative, shear turbulence [8,9], may not be appropriate for this purpose because the scaling laws are different from those of isotropic turbulence. This leads to inconsistencies when mapping the initial conditions of the shear turbulence experiments onto the phase diagrams. Furthermore, flames stabilized in a shear region are not in accord with the fundamental physical concept of turbulent eddies penetrating the flame zone. Because shear turbulence is generated within the flame zone, significant changes in flame wrinkle scales are observable as the shear/flame region evolves (see schlieren records of References 8 and 9). Moreover, the definition of the incident turbulence intensity for the shear flame is ambiguous and may be meaningless.

Clearly, a better experimental methodology is needed to investigate whether or not non-flamelet behavior occurs in an intense turbulent field. The ideal configuration is one in which a steady flame zone propagates into intense isotropic turbulence and can operate in a wide range of mixture and turbulence conditions. The turbulence intensity should also be uniform across the flame brush. Our recently developed weak-swirl burner [10,11] which produces stable, adiabatic and almost planar flames satisfies many of these criteria and can be exploited for this purpose. The weak-swirl generates a divergent flow region where the flame is stabilized. Flame flash-back and blow-off are effectively prevented because the flow velocity upstream of the flame zone is higher than the flame speed and the flow velocity downstream is lower. To generate intense turbulence, we adopted the turbulence generator developed by Videto and Santavicca [12]. Velocity and scalar statistics were measured by two component laser Doppler anemometry and Rayleigh scattering. The use of these diagnostics to determine the flame structure is a significant improvement over ion-probes and thermocouples.

Experimental Apparatus and Diagnostics

The schematic of the swirl burner is shown in Fig 2. The burner consists of a settling chamber, a turbulence generator which incorporates a converging nozzle, and a 50 mm diameter, 233 mm long tube section where the swirler is attached. The turbulence

generator is an adaptation of the linear slot design of Videto and Santavicca [12] to circular geometry. It has a a 0.8 mm wide 107 mm diameter axisymmetric slot. Premixed CH_4/air flow passes through this slot and impacts with a converging nozzle (contraction ratio = 7) which breaks down the large vortical structures generated downstream of the slot. The swirl generator is placed 130 mm above the converging nozzle. It consists of four 2.5 mm diameter , individually adjustable, tangential air jets inclined at 20^o. The swirl rate is monitored by a rotameter which measures the total injection air flow. A 103 mm extension placed above the swirler allows the swirl to developed. The exit rim of the burner is tapered at 45^o to prevent the formation of a recirculation zone above the rim. The swirl number, S, given by Claypole and Syred [13] applies to this burner and its previous version [10] (Table I).

The turbulence characteristics produced by the slot generator are determined by the use of hot-wire anemometry. The results are deduced to determine spectra and length scales. Velocity measurements are made using a four-beam 2-color LDA system [9]. A differential frequency shift of 5 MHz is imposed on both components to remove directional ambiguity. The Doppler signals are analyzed by two TSI frequency counters interfaced with and controlled by a 80386 PC. 4096 co-validated samples are collected using a 10 μsec criterion. Both unconditioned velocities (0.3 μm alumina seeds) and conditioned reactants velocities (silicone oil aerosol seeds) are measured. The LDA seeds are introduced downstream of the turbulence generator to prevent them from clogging the narrow slot. Traversing technique and data reduction are the same as in [10]. The velocity spectra were analyzed by fast Fourier transform (FFT) directly from the LDA analog output with a 6 KHz sampling rate. Silicon oil aerosol is used, so that a high validation rate of at least 10 KHz can be maintained for continuous sampling. To reduce the spectral noise, 100 spectra, each consisting of 4096 samples, were averaged.

For the Rayleigh scattering measurements the laser beam was focused to a 100 μm diameter waist by a 230 mm focal length lens [14]. Scattering from the waist was collected at 90 degrees from the beam direction.. The photomultiplier output was amplified and filtered at 10 KHz. Sampling frequencies were 10 and 20 KHz. The background intensities were also measured and subtracted to obtained the corrected Rayleigh scattering intensity [14].

Results

Burner Operating Range

Even with the intense turbulence, the weak-swirl burner configuration supports a wide range of operating conditions. It is of interest to note that our previous attempts to stabilize v-flames under these intense turbulence condition failed. The lean stabilization limit of $\phi = 0.57$ for CH_4 is the same as that reported by Chan et. al. [10] for a similar burner with a co-flow. That direct injection of swirl air did not change the overall ϕ was confirmed by measuring the oxygen concentration at the center of the flow. Flames could be stabilized with exit velocities ranging from 2 to 7 m/s and higher (the exit velocities are for flow without swirl) with u' vary from 0.52 to 1.65 m/s. For a CH_4/air mixture these conditions correspond to u'/S_L from 1.8 to 11 and l_t/d_L varying from 290 to 150 (table I). Using the definitions given earlier for isotropic turbulence, the range of Ka is then from 0.1 to 3.1 and Da from 161 to 14.

The four cases that have been studied in detail (Table I and Figure 1) represent a systematic approach for investigating the structure of flames with $Ka > 1$ and $Ka < 1$. Case I corresponds to a corrugated flamelet, the most studied flame regime in different configurations. Case II is at the limit between the corrugated flamelet and the predicted distributed reaction zone regime. Cases III and IV are in the distributed reaction zone regime. We are confident with this classification because the incident turbulence is isotropic and fully developed (see next section). For cases III and IV to be in the corrugated flamelet regime, their integral length scales have to be 66 and 148 mm respectively. This is not physically possible because these values are larger than the burner tube diameter.

Turbulence characteristics

Characterizing the incident turbulence and its length scale is essential to our study. Figure 3 shows U, u', v' and $\overline{uv}$ centerline profiles of the isothermal flow for case IV (Table 1). The mean centerline velocity U decreases linearly due to the effect of the swirl which induces centrifugal forces and causes the flow to diverge [10]. The azimuthal velocity component shows that the flow above the burner center is virtually swirl free as in the burner used for previous works [10,11]. The turbulence level is about

23 to 28 % and both u'(x) and v'(x) remain constant. The lack of the turbulence decay is a feature of strained turbulent flow fields. Turbulence generated by the circular slot generator is only slightly anisotropic; a characteristic similar to those generated by perforated plate and grid [15]. The flow is free of shear stress as shown by the low Reynolds stress level. The scaling laws for isotropic turbulence therefore apply to this intense turbulent flow.

Three u' spectra are compared in Figure 4. They are for (1), isothermal flow without swirl, (2), isothermal flow with swirl and (3), reacting flow all under the condition of case IV. The measurement location is 15 mm above the exit just upstream of the turbulent flame brush. The results show that the turbulence generator creates a fully developed turbulent flow with an inertial range. The non-swirling isothermal spectrum is the same as that of grid generated turbulence. Very little difference is found between the isothermal swirling and reactive conditions. The three spectra are essentially identical at frequencies above 50 Hz. Therefore, the swirling motion has no influence on the small scale interactions.

The integral length scale, l_t, was estimated by applying Taylor's hypothesis to the time scales deduced from integrating the auto-correlation functions. For all cases, l_t is about 15 mm. This is due to the fact that at high Reynolds number, l_t is more consistent with the dimension of the burner. The uncertainties in determining l_t are small and do not change the classification of our turbulent flames. Re_t, based on l_t is 1600 (Table I). The turbulent flow is fully developed, having an inertial range, and turbulent length scales ranging from l_t to the Kolmogorov scale, l_k. The values of l_k are also shown in Table I. For cases II and IV l_k are smaller than the reaction zone thickness, d_L. The Kolmogorov scales are deduced based on $l_k/l_t=Re_t^{-3/4}$.

Mean flow structure

Mean flame and flow structures of case IV are presented in Figures 5 and 6. In Figure 5, the U profile decreases linearly away from the burner exit as in the non-reacting profile of Figure 2. Within the flame zone, ($20 < x < 50$ mm), heat release accelerates the flow and generates a plateau. Beyond the flame zone, the velocity resumes its decrease. The rms velocity fluctuations u', v' and the Reynolds stress u'v' are flat and not very different than the non-reacting profiles of Figure 2. This lack of significant change was also found

previously [11] for weak burning lean flames. Under the intense turbulence conditions and mean stretch effects can obscure the flame generated turbulence.

The velocity vectors of Figure 6 are superimposed with contours of the reaction progress variable $\bar{c} = (\rho - \rho_r)/(\rho_p - \rho_r)$ where ρ is the gas density and subscripts r and p represent the reactants and the products. The flow divergence induced by swirl is clearly shown by the velocity vectors of Figure 6. Due to the high injection velocity of the swirl air jets, the flow magnitude is greater at the periphery. A slight flow non-uniformity is also found. This is due to the difficulties in balancing the four swirl jets. As shown by the c contours, flame asymmetry is caused by the flow non-uniformity . The 35 mm flame brush thickness of case IV is larger than the other cases (Table I). These flames are about two times thicker that those generated in the previous burner [11,15].

Turbulent flame speed

An examination of the flame speed data available to date shows that all high turbulence results have been obtained in unsteady 'bomb' experiments [16]. The maximum turbulence attained in open systems is only about $u'/S_L = 4$. The turbulent flame velocities, S_T, in our burner will indicate if steady and unsteady turbulent flame speeds are consistent. The velocity vectors in Figure 6 shows that the flow at the centerline is quite normal to the flame brush. The reactant conditioned velocities at the leading edge ($\bar{c} = 0.05$), can therefore be considered as the turbulent flame speed [11]. Because the changes in the velocity profiles near $\bar{c} = 0.05$ are small, the uncertainties of the results are also small.

Listed in the table I and shown on the figure 7 are the results deduced for our flames. Also shown are the result obtained previously with lower turbulence [11]. S_T for case I overlaps previously results and S_T of cases II to IV show linear increase which seems to be an extension of the data a lower q'/S_L. Compared to the results of Bradley [16], our flame speeds are much higher and shows no sign of leveling off to an asymptotic value. Bradley [16] attributed the asymptotic behavior to stretch effects leading to flame extinction. The stretch rates, K, according to Bradley [16] are shown in Table I. The values of K for cases III and IV would indicate extinction . The flame speed for these cases are almost twice that of Bradley's [16]. These differences in the flame speed strongly suggest the need for continuing investigation of steady and unsteady flame speeds.

The flame structure

The pdfs of the normalized Rayleigh signal is a convenient means to infer the changes of the flame structure. In the wrinkled laminar flame regime, the pdfs are bimodal with the two peaks corresponding to the reactants and the products. The probability of the reactive states, corresponding to the transition between the reactant and burnt gas is small. For flames with a distributed reaction zone, the small scales of the turbulence modify the transport within the reactive states. The expectation is that the probability of encountering the reactive states would be higher, diminishing the distinct bi-modal feature.

The pdfs of cases I and IV for different values of c are compared in Figure 8. They are clearly bimodal and the probability of encountering the reacting states is not any higher for case IV than for case I. The pdfs for the other two cases are also bimodal. These results show that combustion reactions still occur in layers that are relatively thin compared to the turbulent flame zone thickness and there is no drastic change in flame structures at Ka $\approx$ 1. However, they do not imply that distributed reaction zones do not exist nor occur in our flames. It is an accepted view that the modification of the reaction zone begins with the small turbulence eddies penetrating the reaction zone. This has been demonstrated by Gökalp et. al. [7] where only small scale turbulence was generated. In isotropic turbulence, these small turbulent scales co-exist with a broad range of turbulent scales. The large turbulent eddies would wrinkle rather than penetrate the flamelet. Accordingly, even if the flamelet is broadened by a factor of two or three, the probability of the reactive states shown on the pdf of point Rayleigh measurement would remain small. This suggests that a more sophisticated technique such as two point Rayleigh [14] or planar imaging would provide more definitive answers. We plan to continue by extending point Rayleigh measurements to 2-D planar imaging.

Discussion

Currently, there are two theoretical works which describes the transition of flamelet regime to distributed reaction zone regime. First, as proposed by Borghi [5], the Klimov-Williams criterion does not imply a drastic modifications of the flame front structures, especially for the conditions close to Ka =1. Second, as suggested by Poinsot et al. [17] the flame front maybe more resistant to turbulence and the distributed reaction domain boundary in the Borghi plot may shift to a higher value of Ka. Due to the rapid

increase in temperature within the preheat zone, which is 4 to 6 time greater than d_L [17,18], small turbulence eddies can dissipated rapidly and will not modify the reactive zone [17]. Our results are in qualitative agreement with both concepts which shows that flamelet like behavior exists for flames with Ka > 1

Based on the theoretical analyses and our experimental observations, we postulate that the evolution of flamelets into a distributed reaction zone in isotropic turbulence may involve a transitional regime. Cases III and IV fall in this transitional regime close to Ka = 1. The flame structures can be represented by a locally broadened reaction layer. If only the curvature effects are considered, when the flame front is concave to the reactant, it is subjected to negative stretch and the flame front can become thicker. This effect has been demonstrated in numerical and experimental studies of conical flame tips [19]. When the flame front is convex to the reactant, the opposite may occurs depending on the relative effects of local aerodynamic and turbulence stretch. Whether or not the flame front becomes more or less sensitive to the small scales of turbulence is unclear.

Our study has been useful in providing a better understanding of the overall behavior of premixed turbulent flames in intense turbulence. This knowledge will be used to guide our future work to determine the flame structure. Because of the unique attributes of the weak-swirl burner, the experimental conditions can extended to even higher turbulence intensities to test the concept proposed by Poinsot [17].

Conclusion

A technique to stabilize a premixed flame in intense isotropic turbulence without mean shear has been developed. The burner uses a slot type turbulence generator first developed by Videto et al. [12]. The flames are stabilized by weak-swirl generated by air injection upstream of the exit [10]. The turbulence is shown to be isotropic and reaches a high level of 1.5 m/s rms with an integral length scales about 15 mm. Flow divergence created by weak swirl produces stable premixed turbulent flames under a wide range of mixture conditions and turbulence intensities. Four flames are studied. They are designed to investigate systematically the variation in flame structures near the Klimov-Williams criterion of Ka = 1 according to the classifications expressed on the Borghi-Barrère diagram. Case I corresponds to the corrugated flame regime. Case II is at the limit between the corrugated and distributed reaction zone regime. Cases III and IV are in the distributed reaction zone regime.

Measurements of the velocity statistics show that the flames in all the four cases produce very little changes in the mean and rms velocities. The high incident turbulence level seems to have obscured the flame acceleration induced by the heat release and flame generated turbulence. The flame speed is found to increase linearly with turbulent kinetic energy and is much higher that Bradley's [16] unsteady flames results. The high values of stretch, K, found for cases III and IV correspond to extinction conditions of Bradley's unsteady flames.

The pdfs deduced from point Rayleigh scattering data are distinctly bi-modal for all four cases. The probabilities of the reacting states (i.e. contributions from within the reaction zone) are not increased in cases III and IV which are suposedly within the distributed reaction zone regime. This suggest that the Klimov-Williams criterion under-predicts the resilience of wrinkled flamelets to intense turbulence.

Acknowledgment

This work was supported by the Director, Office of Energy Research, Office of Basic Energy Sciences, Chemical Sciences Division of the U. S. Department of Energy under Contract No. DE-AC-03-76SF00098. This visit of the first author to LBL is sponsored by the French Research Ministry. The authors would like to thank Dr. I. G. Shepherd for valuable discussions and to acknowledge Mr. Gary Hubbard for writing the computer controlled and data reduction software.

References

1. Summerfield, M., Reiter, S. H., Kebely, V., and Mascolo, R. W., *Jet Propulsion* 15:377 (1955).

2. Kovasznay, L. S. G., *Jet Propulsion*, 26:485 (1956).

3. Damköhler, G., *Elektrochem.*, 46:601 (1940). English translation : The Effects of Turbulence on the Flame Velocity in Gas Mixtures. N.A.C.A. TM. p. 1112 (1947).

4. Bray, K. N. C., *Turbulent Reacting Flows*, Editors: P. A. Libby and F. A. Williams, Springer, Berlin, 1980, pp. 115.

5. Borghi, R. On the Structures and Morphology of Turbulent Premixed Flames, Recent Advances in the Aerospace Sciences. Editor : Forradi Casci, Plenum, 1985, pp. 117-138.

6. Peters, N., *21st Symposium (Int'l) on Combustion, The Combustion Institute*, Pittsburgh, 1986 pp. 1231-1250.

7. Gökalp, Dumas, G. M. L., Ben-Aim, R. I., *18th Symposium (Int'l) on Combustion*, The Combustion Institute, Pittsburgh, 1981, pp. 969 - 976.

8. .Furukawa, J., Harada, E., and Hirano, T., *23rd Symposium (Int'l) on Combustion*, The Combustion Institute, Pittsburgh, 1992, pp. 789-794.

9 Yoshida, A., Narisawa, M., and Tsuji, H., *24th Symposium (Int'l) on Combustion*, The Combustion Institute, Pittsburgh, 1992, pp. 519-525.

10. Chan, C. K., Lau, K. S., Chin, W. K., and Cheng R. K., *24th Symposium (Int'l) on Combustion*, The Combustion Institute, Pittsburgh, 1992, pp. 511-518.

11. Cheng, R. K. : Velocity and Scalar Statistics of Premixed Turbulent Flames Stabilized by Weak-Swirl, submitted to Combustion and Flame (1993).

12. Videto, B. D., and Santavicca, D. A. *Combustion Science and Technology*, 76:159-164 (1991).

13. Claypole T. C. and Syred N. *18th Symposium (Int'l) on Combustion*, The Combustion Institute, 1981, p. 81.

14. Cheng, R. K., Bill, R. G., Jr. and Robben, F., *Eighteenth (Int'l) Symposium on Combustion*, The Combustion Institute, Pittsburgh, 1981, pp. 1021-1029.

15 Cheng, R. K., and Shepherd, I. G., Combustion and Flame, 85 : 7 (1991).

16. Bradley, D., *24th (Int'l) Symposium on Combustion*, The Combustion Institute, Pittsburgh, 1992 pp. 247-262

17. Poinsot, T., Veynante, D. and Candel, S., *23rd (Int'l) Symposium on Combustion*, The Combustion Institute, Pittsburgh, 1990 pp. 613-619

18 Jarosinski, J., Combustion and Flame, 56 : 337 (1984).

19 Poinsot, T., Echekki, T. and Mungal, M. G., Combustion Science and Technology, 81 : 45 (1992).

Table I Experimental Conditions and Relevant Parameters

Case	I	II	III	IV
Exit velocity without swirl (m/s)	2.00	3.00	5.00	7.00
Flow rate (l/s)	-	7.1	12.7	17.
Swirl number, S	-	0.09	0.08	0.06
Equivalence ratio, ϕ	0.80	0.65	0.60	0.60
Laminar flame speed, S_L(m/s)	0.30	0.18	0.15	0.15
Reaction zone thickness, d_L(μm)	51.7	83.8	97.6	97.6
u' (m/s) at c = 0.05	0.52	0.89	1.30	1.70
v' (m/s) at c=0.05	0.53	1.00	1.00	1.25
q (m/s) at c= 0.05	0.37	0.67	0.82	1.06
Integral length scale, l_t (mm)	15.00	15.00	15.00	15.00
Turbulent Reynolds number, Re_l	488	835	1220	1594
Kolmogorov scale, l_k (μm)	144	96	73	59
l_t/d_L	290	179	154	154
u'/S_L	1.8	5.0	8.8	11.5
Damköhler number, Da	165	36	18	13
Karlovitz number, Ka	0.1	0.8	2.1	3.1
Turbulent flame thickness, d_T (mm)	26.70	25.50	26.00	35.00
Turbulent flame speed, S_T (m/s)	1.4	1.8	2.7	3.6
q'/S_L	1.3	3.7	5.5	7.1
S_T/S_L	4.7	10.3	18.1	24.5
Stetch rates defined by Bradley [15] $K = 0.157\ (u'/S_L)^2\ Re_l^{-0.5}$	0.023	0.14	0.35	0.52

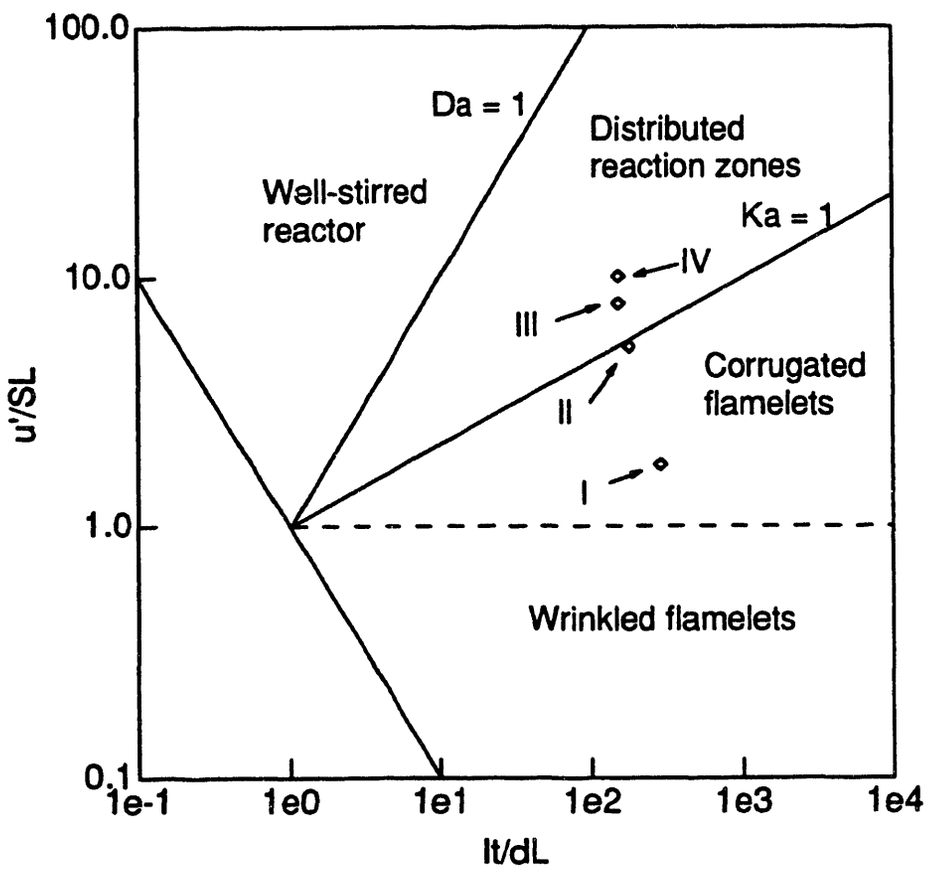

Figure 1: Classification of the cases on the Borghi diagram [5].

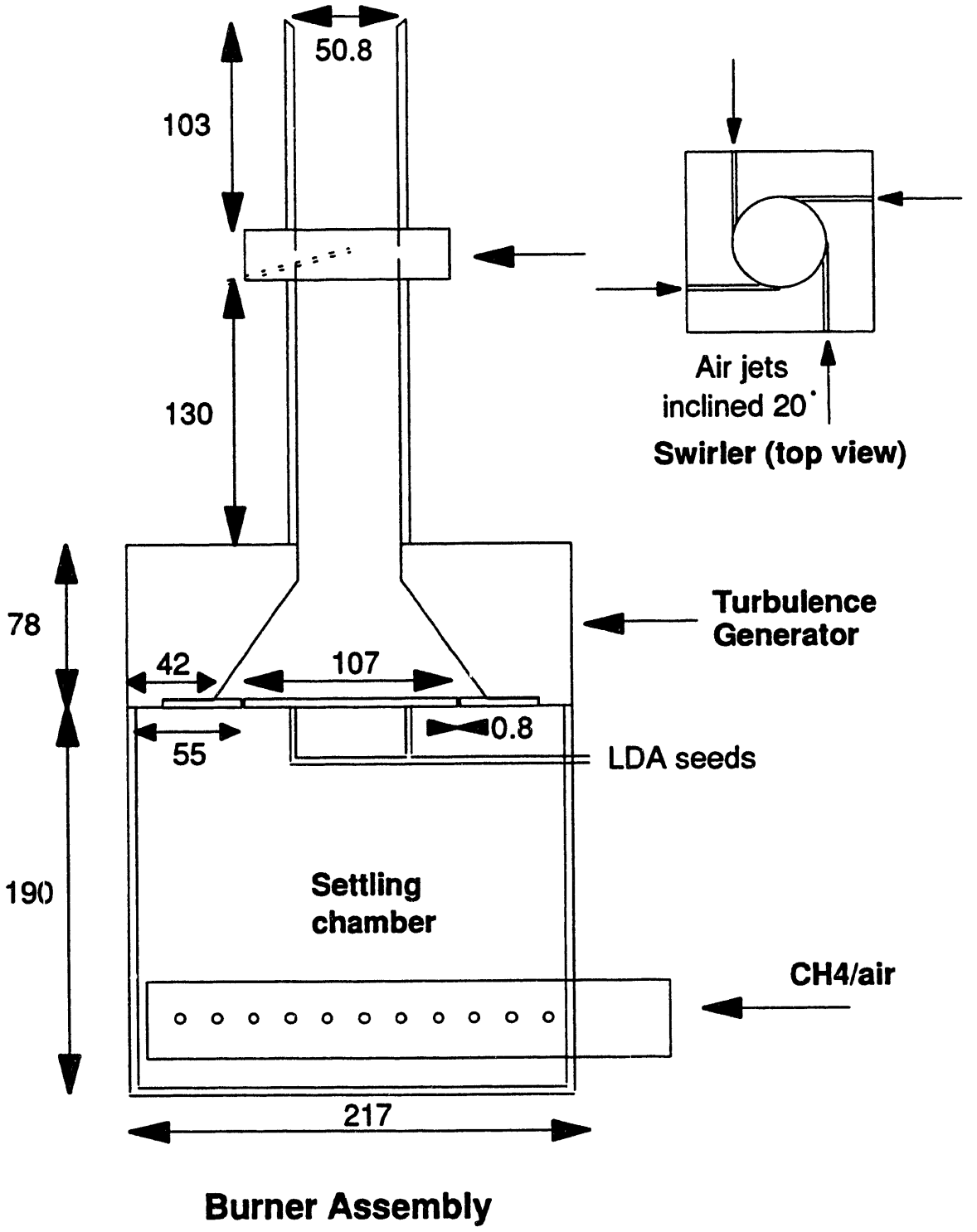

Figure 2 : Burner schematic

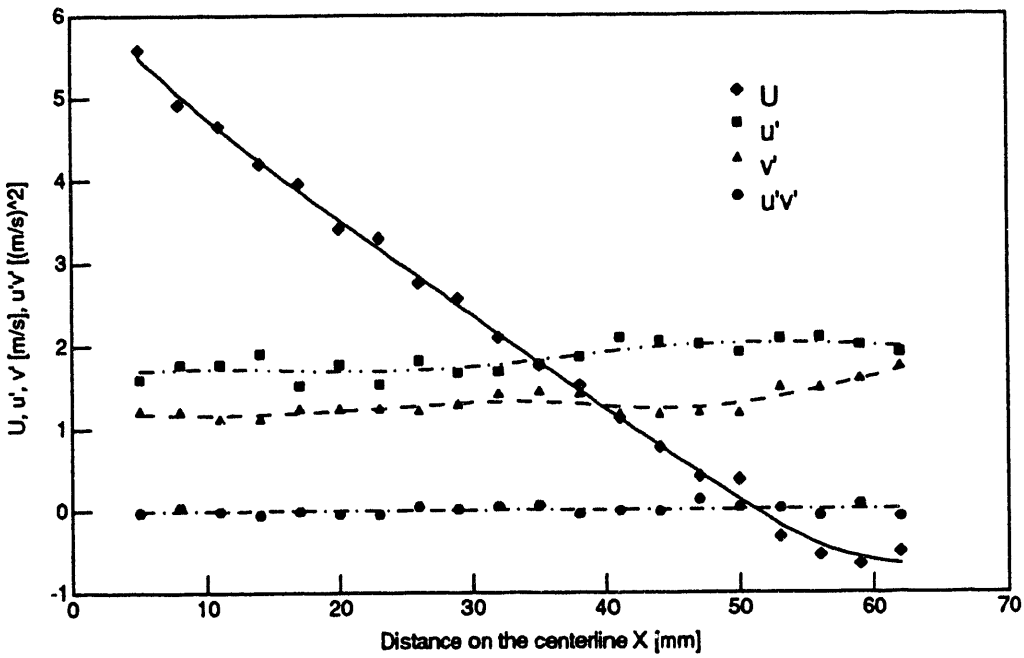

Figure 3 : Centerline velocity profiles for the case IV with isothermal conditions

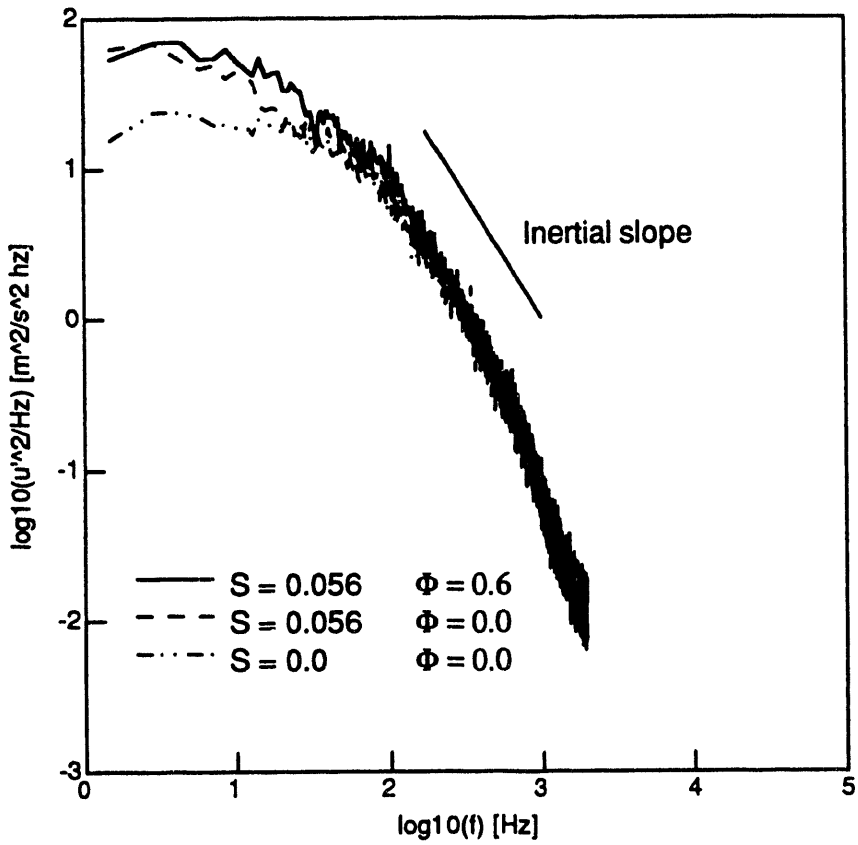

Figure 4 : Axial velocity spectra for the case IV at 15 mm of the exit

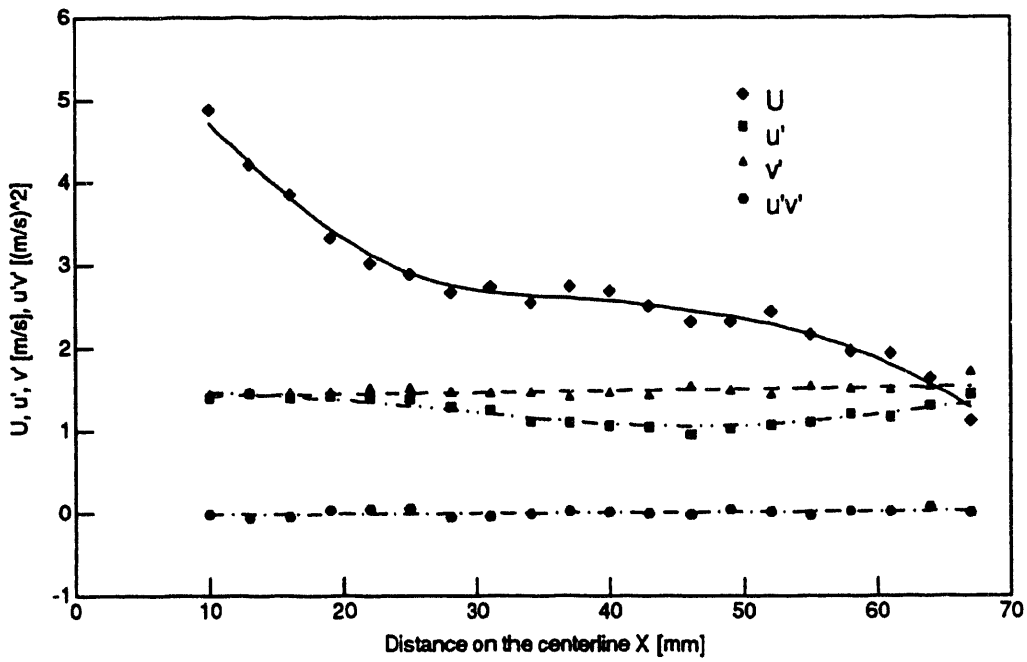

Figure 5 : Centerline velocity profile of the unconditioned velocity for the case IV

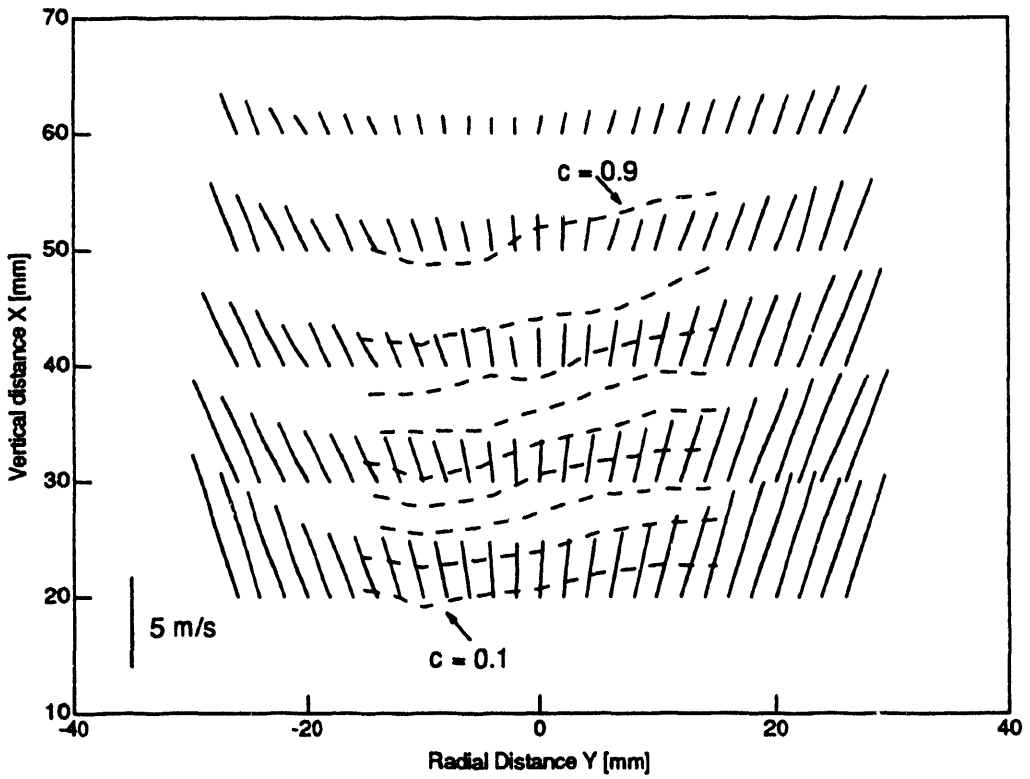

Figure 6 :Two dimensional velocity vectors measured for the case IV and C contours

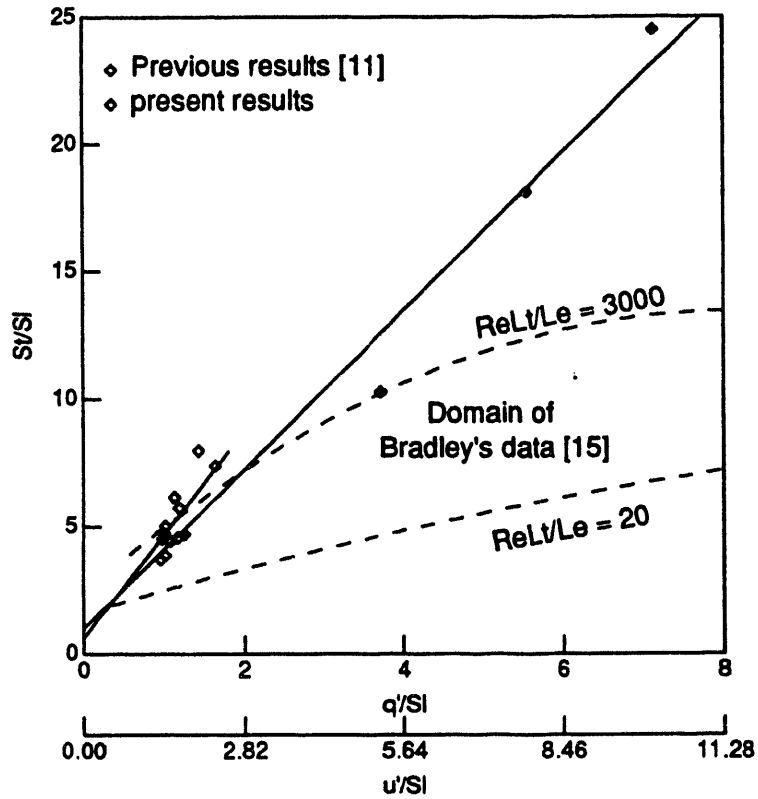

Figure 7 : Correlation of the burning rate ratio and the turbulent/laminar speed ratio.

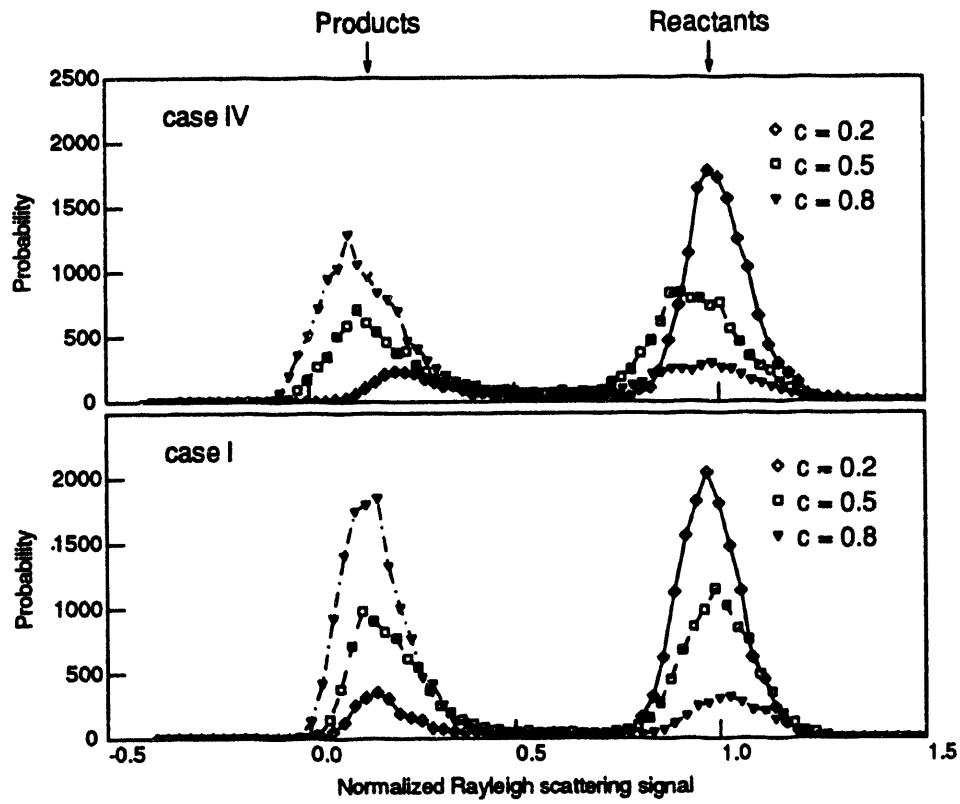

Figure 8 : Normalized Rayleigh pdf for the cases I and IV

DATE

FILMED

9/9/94

END